

1 **Identification of magnetic anomalies based on ground**
2 **magnetic data analysis using multifractal modeling: A case**
3 **study in Qoja-Kandi, East Azerbaijan Province, Iran**

4

5 **E. Mansouri¹, F. Feizi², and A. A. Karbalaei Ramezanali¹**

6 [1]{Young Researchers and Elite Club, South Tehran Branch, Islamic Azad
7 University, Tehran, Iran}

8 [2]{Mine Engineering Department, South Tehran Branch, Islamic Azad University, Tehran,
9 Iran}

10 Correspondence to: F.Feizi (feizi.faranak@yahoo.com)

11

12 **Abstract**

13 Ground magnetic anomaly separation using Reduction-To-the-Pole (RTP) technique and the
14 fractal concentration-area (C-A) method has been applied to the Qoja-Kandi prospepecting area
15 in NW Iran. The geophysical survey resulting in the ground magnetic data was conducted for
16 magnetic elements exploration. Firstly, RTP technique was applied for recognizing
17 underground magnetic anomalies. RTP anomalies was classified in to different populations
18 based on the current method. For this reason, drilling point areas determination by RTP
19 technique was complicated for magnetic anomalies, which is in the center and north of studied
20 area. Next, C-A method was applied on the RTP-Magnetic-Anomalies (RTP-MA) for
21 demonstrating magnetic susceptibility concentrations. This identification was appropriate for
22 increasing the resolution of the drilling point areas determination and decreasing the drilling
23 risk issue, due to the economic costs of underground prospecting. In this study, the results of
24 C-A Modeling on the RTP-MA are compared with 8 borehole data. The results shows that there
25 is a good correlation between anomalies derived via C-A method and log report of boreholes.
26 Two boreholes were drilled in magnetic susceptibility concentrations, based on multifractal
27 modeling data analyses, between 63533.1 to 66296 nT. Drilling results showed appropriate

1 magnetite thickness with grades greater than 20% Fe. Total associated with anomalies
2 containing andesite units host iron mineralization.

3 **1 Introduction**

4 Mineral exploration aims at discovering new mineral deposits in a region of interest (Abedi et
5 al., 2013). These mineral deposits could be related to magnetic anomalies which are situated
6 within underground. In the first step of identification underground magnetic anomalies, few
7 boreholes should be drilled after interpretation Ground magnetic data. Obviously, using new
8 methods could increase the resolution of the drilling point areas determination and decrease the
9 drilling risk. A cursory look at magnetic maps would present more information about the shape
10 of such a buried features. However, the information acquired from map can provide additional
11 details about the specification of underground magnetic anomalies especially exact locations.
12 Magnetic anomaly depends on the inclination and declination of the body's magnetization
13 generally. Also we know that the orientation of the magnetic body depends to magnetic north.
14 According to the mentioned issues (Baranov, 1957) and (Baranov and Naudy, 1964) proposed
15 a mathematical approach known as reduction-to-the-pole (RTP) for simplifying anomaly shape
16 and determining anomaly exact location. As a result of increasing the resolution of RTP
17 technique, concentration-area (C-A) fractal method was applied. Fractal geometry is a Non-
18 Euclidean geometry established by Mandelbrot (1983) and has been applied in geosciences and
19 mineral exploration, especially in geophysical and geochemical exploration since 1980s,
20 (Turcotte (1989), Bolviken et al. (1992), Korvin (1992), Cheng et al. (1994), Agterberg et al.
21 (1996), Cheng (1999), Turcotte (2004), Dimri (2005) and Shen et al. (2009)).

22 In this study, concentration-area (C-A) fractal method was used to gridded RTP data set, for
23 better classification of RTP map which generated from RTP technique. This procedure was
24 applied to the ground magnetic data of Qoja-Kandi, Zanjan Province, Iran.

25

26 **2 The concentration-area fractal method**

27 The concentration-area (C-A) method serves to illustrate the correlated relationship between
28 the obtained results. Its most useful features are the easy implementation and the ability to
29 compute quantitative anomalous thresholds (Cheng et al., 1994).

1 Cheng et al. (1994) proposed the concentration–area (C–A) method for separating geochemical
2 anomalies from background in order to characterize the distribution of elemental
3 concentrations. Equations (1) Shows the general form of this model.

4 $A(\rho \leq \gamma) \propto \rho^{-a_1}; A(\rho \geq \gamma) \propto \rho^{-a_2}$ (1)

5 Where $A(\rho)$ denotes the area with concentration values greater than the contour value ρ ;
6 γ represents the threshold; and a_1 and a_2 are characteristic exponents. The breaks between
7 straight line segments in C-A log-log plot and the corresponding values of ρ are known as
8 thresholds to separate geophysical values into different components representing different
9 causal factors such as, lithological differences, geochemical processes and mineralizing events
10 (Lima et al., 2003). Thus, applying C-A fractal model to the geochemical data, improves
11 resolution of the data helping to explore the deposits. It seems that, applying this model to
12 ground magnetic data improves the accuracy of magnetite deposit exploration. The most useful
13 feature of the C-A method is its capability to compute anomaly thresholds (Goncalves et al.,
14 2001). Using fractal theory, Cheng et al. (1994) derived similar power-law relationships and
15 equations in extended form. The area $A(\rho)$ for a given ρ is equal to the number of cells
16 multiplied by cell area with concentration values greater than ρ . Average concentration values
17 are used for those boxes containing more than one sample. Area-concentration [$A(\rho)$] with
18 element concentrations greater than ρ usually shows a power-law relation (cheng et al., 1994).

19 **3 The study area and geological setting**

20 The Qoja-Kandi area is located within the Orumieh-Dokhtar magmatic arc in northwest of
21 Iran (Fig. 1); This magmatic arc is the most important exploratory area for metals, and hosts
22 the majority of the larger metals deposits such as copper and iron (Hassan-Nezhad and Moore,
23 2006) The investigated area characterized by Precambrian to Jurassic units and Oligo-Miocene
24 volcanic rocks. Different types of metal ore deposits, such as iron have already been
25 documented near studied area. The lithology of this part includes schist and shale (Kahar
26 formation), dolomite and limestone (Elika formation), shale, sandstone and limestone
27 (Shemshak formation), limestone, marl, sandstone, conglomerate and andesit. A magnetite
28 dyke which has outcrops in andesite units has already been seen near studied area. It seems that
29 this magnetite dyke presence in Qoja-Kandi area.

30

4 Ground magnetic data analysis

Ground magnetic data are acquired in the region at 15 m spacing along lines in the north direction and spaced 10 m apart. 6997 geophysical ground data were collected by GSM-19T proton. GSM-19T proton magnetometer has absolute accuracy +/- 0.2 nT.

4.1 The TMI anomaly map

The Total-Magnetic-Intensity (TMI) map of the Qoja-Kandi area was obtained to delineate the subsurface anomaly. Fig. 2 indicates TMI with ground magnetic data points. The ground magnetic anomalies range from 38633 to 69509 nT and are characterized by both low and high frequencies of anomalies. The map reveals that dipolar (anomalies having positive and negative components) magnetic anomalies have a general E-W direction, which is in the center and north of studied area. There are three obvious dipolar magnetic anomalies (two anomalies in the east and west of the center and one anomaly in the north) in the Qoja-Kandi prospecting area which are expected to depend on two magnetite dyke in andesite units.

4.2 Reduction to the pole technique

A difficulty in interpretation with TMI anomalies is that they are dipolar (anomalies having positive and negative components) such that the shape and phase of the anomaly depends on the part of magnetic inclination and the presence of any remanent magnetization. Because of depending magnetic anomaly on the inclination and declination of the body's magnetization, the inclination and declination of the local earth's magnetic field, and the orientation of the body with respect to magnetic north, (Baranov, 1957) and (Baranov and Nudy, 1964) proposed a mathematical approach known as reduction to the pole for simplifying anomaly shape.

The reduction-to-the-pole (RTP) technique transforms TMI anomalies to anomalies that would be measured if the field were vertical (assuming there is only an inducing field). This RTP transformation makes the shape of magnetic anomalies more closely related to the spatial location of the source structure and makes the magnetic anomaly easier to interpret, as anomaly maxima will be located centrally over the body (provided there is no remanent magnetization present). Thus, the RTP reduces the effect of the Earth's ambient magnetic field and provides a more accurate determination of the position of anomalous sources. It is therefore understood that the total magnetization direction is equivalent to that of the current inducing field.

1 Before applying the methods, the total field anomaly data were converted to RTP using a
2 magnetic inclination of 55.43° and a declination of 4.93° . RTP anomalies, shows three obvious
3 magnetic anomalies (two anomalies in the east and west of the south and one anomaly in the
4 north) in the studied area, elongated in approximate E-W direction. The highest class of RTP-
5 Magnetic-Anomalies (RTP-MA) based on Reduction to the pole technique is > 55370.7 nT with
6 24941.79 square meters area. Also, RTP anomalies was classified to different populations based
7 on this method, as illustrated in Fig. 3. Based on this method, drilling points determination with
8 RTP technique was complicated.

9 **4.3 Application of C-A Modeling on the RTP-MA**

10 Multifractal models are utilized to quantify patterns such as geophysical data. Fractal and
11 multifractal modeling are widely applied to distinguish the different mineralized zones (Cheng,
12 2007). Multifractal theory could be interpreted as a theoretical framework that explains the
13 power law relationships between areas enclosing concentrations below a given threshold value
14 and the actual concentrations itself. To demonstrate and prove that data distribution has a
15 multifractal nature, an extensive computation is required (Halsey et al., 1986). This method has
16 several constrains especially when the boundary effects on irregular geometrical data sets are
17 involved (Agterberg et al., 1996; Goncalves, 2001; Cheng, 2007; Xie et al., 2010). Multifractal
18 modelings in geophysical and geochemical exploration help to find exploration targets and
19 mineralization potentials in different types of deposits (Yao and Cheng, 2011). The C-A method
20 seems to be equally applicable to all cases which means that geophysical distributions mostly
21 satisfy the properties of a multifractal function. There is some evidence that geophysical and
22 geochemical data distributions have fractal behavior in nature, e.g. Bolviken et al. (1992),
23 Turcotte (1997), Goncalves (2001), Gettings (2005) and Li and Cheng (2006). This theory
24 improves the development of an alternative interpretation validation and useful methods to be
25 applied to geophysical distributions analysis.

26 In this study, 57307 transformed RTP data were processed for identification of magnetic
27 anomalies. Statistical results reveal that RTP-MA mean value is 48441 nT, as depicted in Fig.
28 4, and the RTP-MA domain shows a wide range. **C-A Modeling overcomes the distortion effects**
29 **of outliers on the traditional techniques and makes it unnecessary to determine whether the concentration**
30 **data are drawn from a normal (i.e., Gaussian) distribution or log-normal distribution, and this advances**
31 **the analysis resolution of anomalies (Fig. 5).** RTP-MA distribution map was generated with
32 minimum curvature method. The estimated RTP-MA model in terms of RTP data values was

1 intended to build of the C-A log-log plot for RTP-MA. Based on linear segments and
2 breakpoints log-log plot, as shown in Fig. 6, geophysical population were divided. RTP
3 threshold values are 45383, 47424.2, 49493.7, 56493.7 and 635331.1 which are very low, low,
4 moderate, high and very high intensity anomaly threshold values, respectively, as illustrated in
5 Table 1. **Pairs of estimated exponents and corresponding optimum thresholds for RTP-MA are**
6 **presented in Table 2. The thresholds delineate anomalous areas. Comparison of the areas above**
7 **and below the threshold of 6022 nT on the contour map (Fig. 3) with the RTP map shows**
8 **significant spatial correlation between the areas with RTP-MA concentration above 6022 nT.**

9 These geophysical populations were determined based on the breakpoints in log-log plot.
10 Actually the length of the tangent, demonstrate the extents of geophysical populations in fractal
11 model. It is mentioned that the number of population in fractal model could be more or less
12 than five, but actually the extent of the last class population isn't highly dependent on the
13 number of population in fractal model. Hence, there are five populations for RTP-MA which
14 illustrate that fifth class of RTP-MA based on fractal method is > 63533.1 nT with very high
15 priority for drilling. Consequently, the locations of RTP-MA (two anomalies) based on fractal
16 method are situated in the east of southern part of the area, as depicted in Fig. 7.

17 **5 Control with borehole data**

18 A method of investigating subsurface geology is, of course, drilling boreholes. For a more
19 accurate results about identification of magnetic anomalies, the results of C-A Modeling on the
20 RTP-MA are compared with borehole data (Table 3). There are 8 drilled boreholes in this area
21 that are used for identification of magnetic anomalies obtained from boreholes (Fig. 8). The
22 drilled boreholes were analyzed and studied by geologists. Hence, range of magnetite ores in
23 each borehole were obtained and documented as log report in Table 3. The accepted lower limit
24 for the ore length, is the grade 20% Fe total.

25 RTP transformed data based on ground magnetic anomaly data collected from C-A moderate
26 anomalies in Qoja-Kandi prospecting area show magnetic susceptibility concentration between
27 63533.1 to 66296 nT with 1957.64 m^2 area. This study shows that the areas with very high
28 priority obtained by C-A method have magnetite concentration with appropriate thickness. This
29 point is significant that borehole 1 and 2 were drilled in mentioned places and confirmed the
30 results of C-A model (Fig. 9) for increasing the resolution of drilling point determination and
31 decreasing the drilling risk. Fig. 9 shows 3D RTP map of Qoja-Kandi based on C-A method
32 with pictures from magnetite zones in the surface of drilled borehole1 and 2, in addition of

1 mentioned boreholes log plots. It is necessary to mention that, the TERRA satellite has a back-
2 looking telescope with a resolution of 15 m in the VNIR that matches with the wavelength of
3 the band 3 that is used to extract 3D information for provided Fig. 9.

4 The results confirmed there is affirmative correlation between anomalies derived via C-A
5 method and log report of boreholes. Furthermore, the ratio of the ore length and total core length
6 is calculated in Table 3. The number of this ratio is between ranges of 0 to 1. Whatever this
7 number is larger and close to 1, the resolution of the drilling point determination increase and
8 the drilling risk decrease. The results shows positive correlation between the ratio of the ore
9 and total core column, and Priority areas for drilling column. Based on this study, anomalies
10 associated with andesite units host iron mineralization. Also, there isn't any mineralization in
11 other geological units such as limestones and conglomerates in northwest of the studied area. It
12 should be noted that, magnetite ores have outcrops in andesite units (Fig. 9).

13 **6 Conclusions**

14 Separation of magnetic anomalies using combine of RTP technique and C-A fractal modelling
15 has been used in Qoja-Kandi prospecting area as a new geophysical method for increasing the
16 resolution of the drilling points determination. This study demonstrates that C-A method
17 utilizing for ground magnetic anomaly separation is an appropriate manner for geophysical
18 prospecting.

19 There was a multifractal model for RTP-MA, based on Log-log plots in the prospecting area. In
20 this paper, RTP anomalies results from C-A method and RTP technique were compared.
21 Anomalies resulting from RTP technique show huge anomalies in three parts, but C-A method
22 show two small anomalies. RTP anomalies based on RTP technique are similar to anomalies
23 from C-A method because of normal distribution in Qoja-kandi area. According to correlation
24 between geological particulars and RTP anomalies obtained from C-A method, andesite units
25 host the anomalies in the studied area.

26 There is an appropriate correlation between the calculated anomalous threshold values and ore
27 thicknesses in total cores. Also, the ratio of the ore length and total core length is related to
28 anomalous threshold, calculated with C-A method. Based on RTP technique, three anomalies
29 (two RTP anomalies were identified in the east and west of the southern part of the area and
30 one anomaly in the northern part). Also, according to the C-A method, two small anomalies are
31 situated in the east of southern part of the prospecting area with very high priority for drilling.

1 Borehole 1 and 2 were drilled in mentioned places and confirmed the results of C-A model for
2 increasing the resolution of drilling point determination and decreasing the drilling risk.

3 Hence study geophysical magnetic anomalies with the C-A method can be a proper way for
4 geophysists to find targets with enriched magnetic elements. Also, applying C-A log-log can
5 increase the resolution of the drilling point determination and decrease the drilling risk.

6

1 **References**

2 Abedi, M., Torabi, S.A., Norouzi, G.H.: Application of fuzzy AHP method to integrate
3 geophysical data in a prospect scale, a case study: Seridune copper deposit, Boll. Geofisica
4 Teorica Appl, 54, 145–164, 2013.

5 Agterberg, F. P., Cheng, Q., Brown, A., and Good, D.: Multifractal modeling of fractures in the
6 Lac du Bonnet batholith, Manitoba, Comput. Geosci., 22, 497–507, 1996.

7 Arian, M.: Physiographic-Tectonic Zoning of Iran's Sedimentary Basins, Open Journal of
8 Geology, 3, 169-177, 2013.

9 Baranov, V., Naudy, H.: Numerical calculation of the formula of reduction to the magnetic
10 pole, Geophysics, 29, 67-79, 1964.

11 Baranov, V.: A new method for interpretation of aeromagnetic maps; pseudo-gravimetric
12 anomalies, Geophysics, 22, 359-382, 1957.

13 Bolviken, B., Stokke, P. R., Feder, J., and Jossang, T.: The fractal nature of geochemical
14 landscapes, J. Geochem. Explor., 43, 91–109, 1992.

15 Cheng, Q., Agterberg, F. P., and Ballantyne, S. B.: The separation of geochemical anomalies
16 from background by fractal methods, J. Geochem. Explor., 51, 109–130, 1994.

17 Cheng, Q.: Multifractal imaging filtering and decomposition methods in space, Fourier
18 frequency, and eigen domains, Nonlin. Processes Geophys., 14, 293–303, doi:10.5194/npg 14-
19 293-2007, 2007.

20 Cheng, Q.: Spatial and scaling modelling for geochemical anomaly separation, J. Geochem.
21 Explor., 65, 175–194, 1999.

22 Dimri, V. P.: Fractal Behavior of the Earth System, The Netherlands, Springer, 208 pp., 2005.

23 Gettings, M. E.: Multifractal magnetic susceptibility distribution models of hydrothermally
24 altered rocks in the Needle Creek Igneous Center of the Absaroka Mountains, Wyoming,
25 Nonlin. Processes Geophys., 12, 587–601, doi:10.5194/npg-12-587- 2005, 2005.

26 Goncalves, M. A., Mateus, A., and Oliveira, V.: Geochemical anomaly separation by
27 multifractal modeling, J. Geochem. Explor., 72, 91–114, 2001.

1 Halsey, T. C., Jensen, M. H., Kadanoff, L. P., Procaccia, I., and Shraiman, B. I.: Fractal
2 measures and their singularities: The characterization of strange sets. *Phys. Rev. A*, 33, 1141
3 1151, 1986.

4 Hassan-Nezhad, A. A., Moore, F.: A stable isotope and fluid inclusion study of the Qaleh-Zari
5 Cu–Au–Ag deposit, Khorasan Province, Iran, *Journal of Asian Earth Sciences.*, 27, 805–818,
6 2006.

7 Korvin, G.: *Fractal Models in the Earth Science*, Elsevier, Amsterdam, 396 pp., 1992.

8 Li, Q. and Cheng, Q.: VisualAnomaly: A GIS-based multifractal method for geochemical and
9 geophysical anomaly separation in Walsh domain, *Comput. Geosci.*, 32, 663–672, 2006.

10 Lima, A., De Vivo, B., Cicchella, D., Cortini, M., and Albanese, S.: Multifractal
11 IDWinterpolation and fractal filtering method in environmental studies: an application on
12 regional stream sediments of (Italy), Campania region, *Appl. Geochem.*, 18, 1853–1865, 2003.

13 Mandelbrot, B. B.: *The Fractal Geometry of Nature*, W. H. Freeman, San Fransisco, 468 pp.,
14 1983.

15 Shen, W., Fang, C., and Zhang, D.: Fractal and Chaos Research of Geomagnetic Polarity
16 Reversal, *Earth Sci. Front.*, 16, 201–206, 2009.

17 Turcotte, D. L.: *Fractals and Chaos in Geology and Geophysics*, Cambridge University Press,
18 Cambridge, 398 pp., 1997.

19 Turcotte, D. L.: Fractals in geology and geophysics, *Pure Appl. Geophys.*, 131, 171–196, 1989.

20 Turcotte, D. L.: The relationship of fractals in geophysics to “the new science”, *Chaos, Soliton.*
21 *Fract.*, 19, 255–258, 2004.

22 Xie, S., Cheng, Q., Zhang, S., and Huang, K.: Assessing microstructures of pyrrhotites in
23 basalts by multifractal analysis, *Nonlin. Processes Geophys.*, 17, 319–327, doi:10.5194/npg 17-
24 319-2010, 2010.

25 Yao, L. and Cheng, Q.: Multi-scale interactions of geological processes during mineralization:
26 cascade dynamics model and multifractal simulation, *Nonlin. Processes Geophys.*, 18, 161–
27 170, doi:10.5194/npg-18-161-2011, 2011.

28

1 Table 1. RTP classification of magnetic anomalies based on fractal method.

2

Class ID	Classes range (nT)	Priority areas for drilling
1	45383 – 47424.2	Very low
2	47424.2 – 49493.7	Low
3	49493.7 – 56493.7	Moderate
4	56493.7 – 63533.1	High
5	63533.1 - 66296	Very high

3

1 Table 2. Results obtained by using the power law method and weights of evidence procedure;
2 α_1 and α_2 are the exponents of the power-law relation for concentration values less and greater
3 than the threshold value (v), respectively.

Total magnetic intensity	v	Power law α_1	α_2	W. of T v
RTP(nT)	60022	0.0116	0.0458	60022

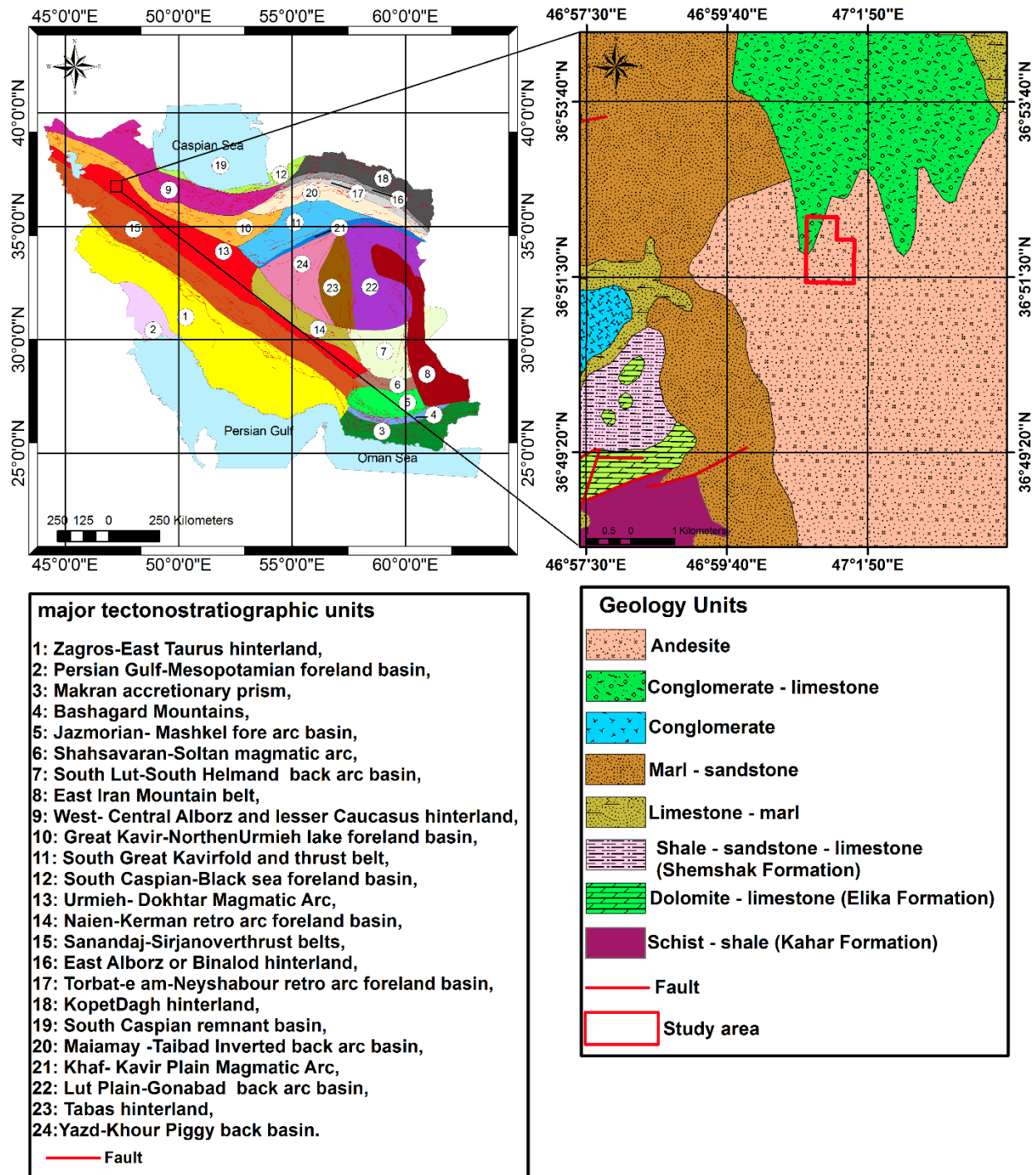
5
6
7
8
9
10
11
12
13
14
15
16
17
18
19
20
21

1 Table 3. Log report of boreholes with RTP classification based on fractal method.

2

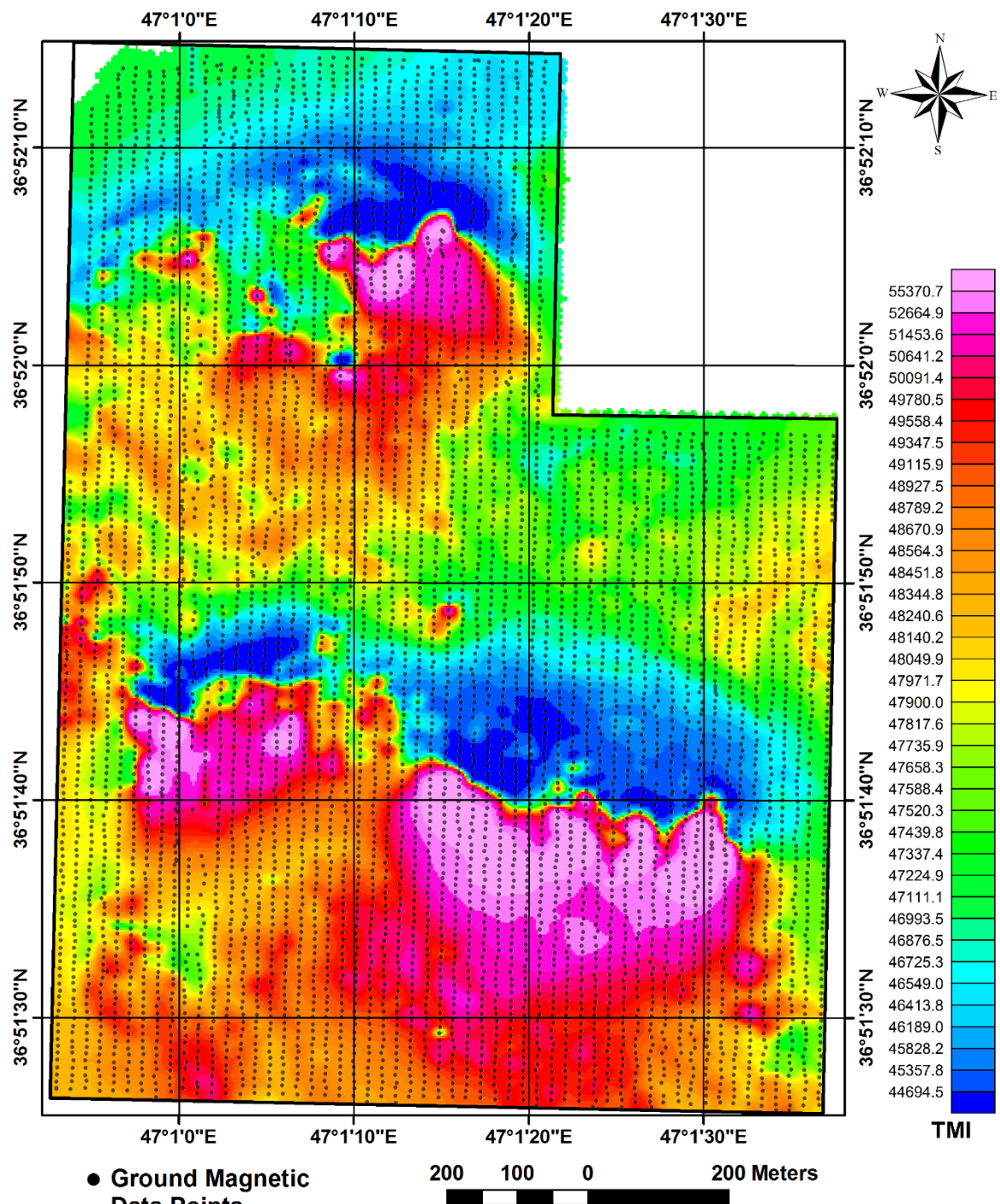
Borehole ID	Total core (m)	Magnetite thickness (m) in total core(grades greater than 20% Fe total)			Magnetite core (m)	Priority areas for drilling
		Ore core	/	Total core		
BH1	136.5	52.4	0.38	19.3	19.3	25.2
					60.7	85.2
					109.4	131.4
BH2	171.2	47.2	0.27	4	4	12.2
					50.2	53.5
					130.6	166.3
BH3	151.2	32	0.21	80	80	102
					112	122
BH4	106	12.5	0.11	44	44	48
					81	89.5
BH5	58.9	0	0	-	-	Very low
BH6	136.5	3	0.02	69	72	Low
BH7	172	14	0.08	44	44	47
					61.5	63.5
					156	164
BH8	157	29	0.18	70	70	90
					133	142

3



1
2
3
4
5

Figure 1. Physiographic-tectonic zoning map of Iran's sedimentary basins (Arian, 2013) and location of study area.



1
2

3 Figure 2. TMI map of Qoja-Kandi with ground magnetic data points.

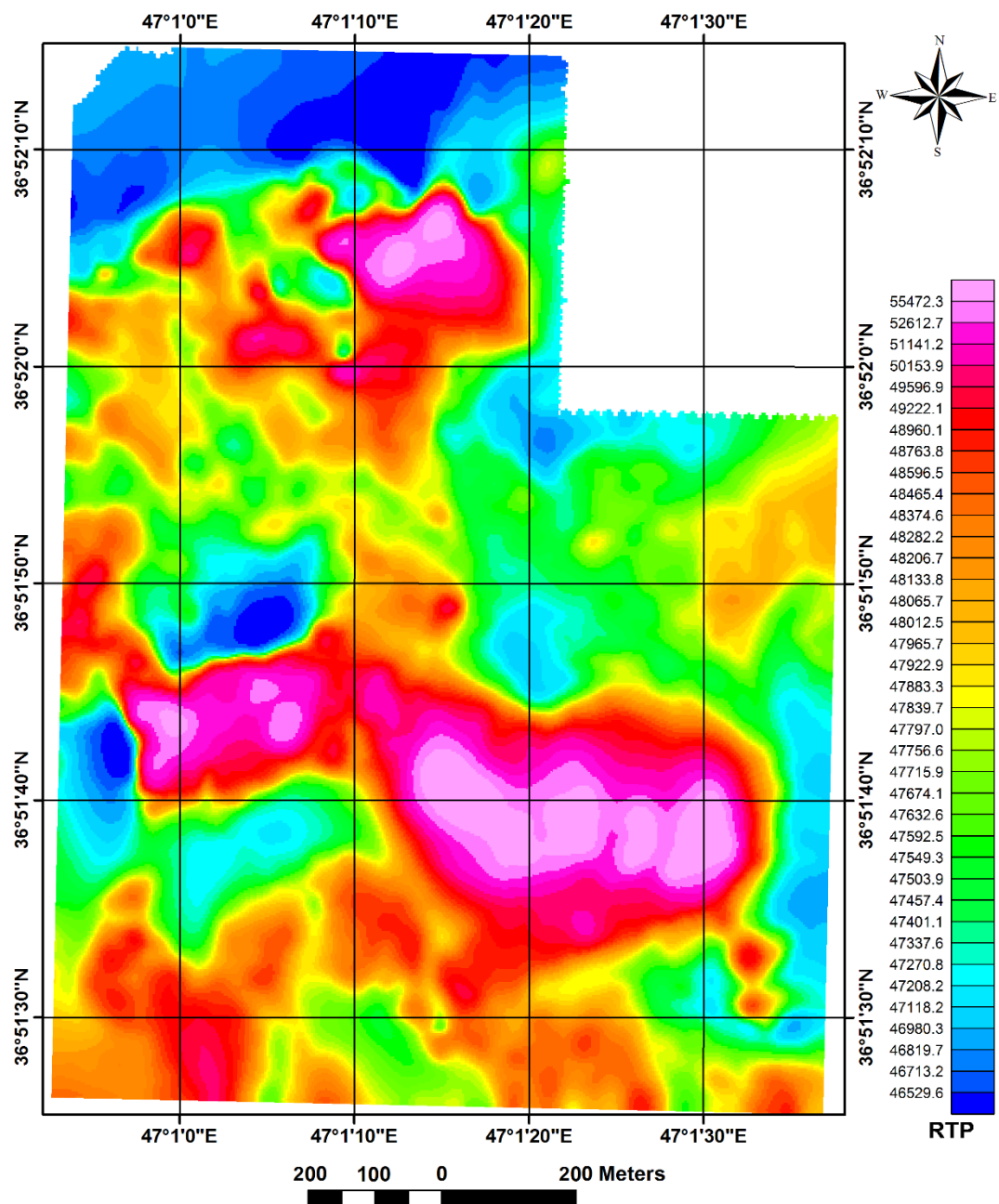
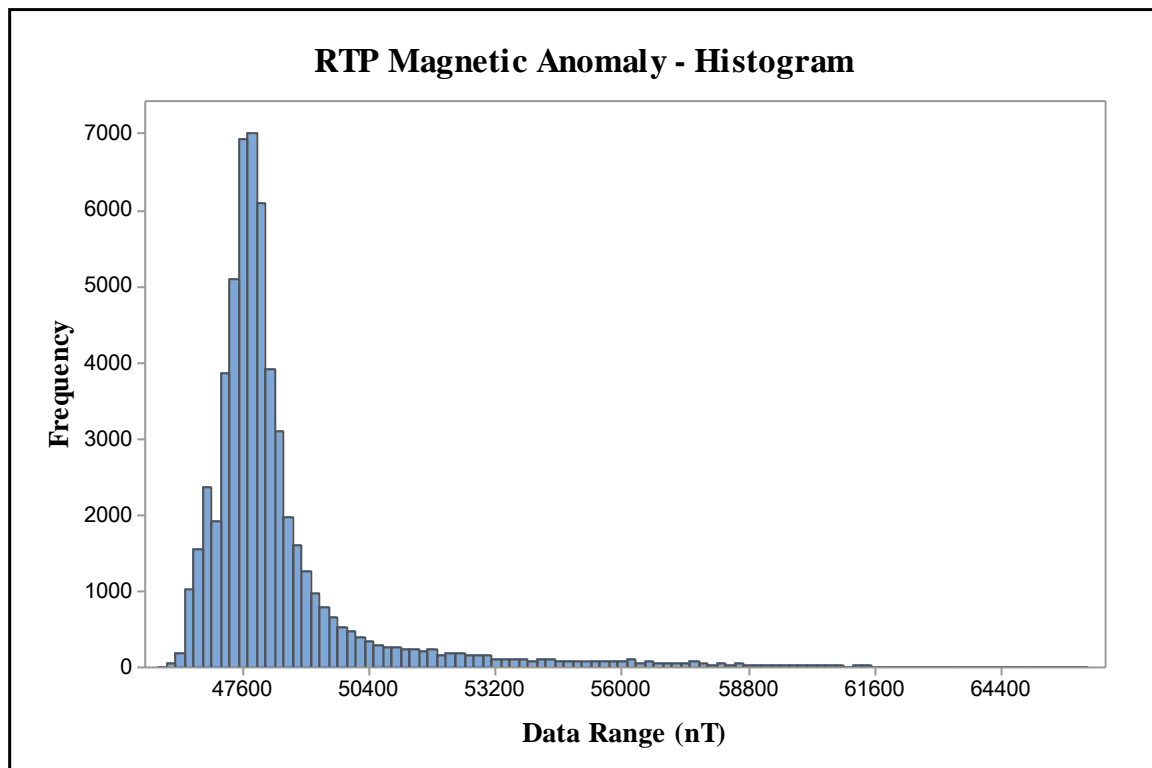


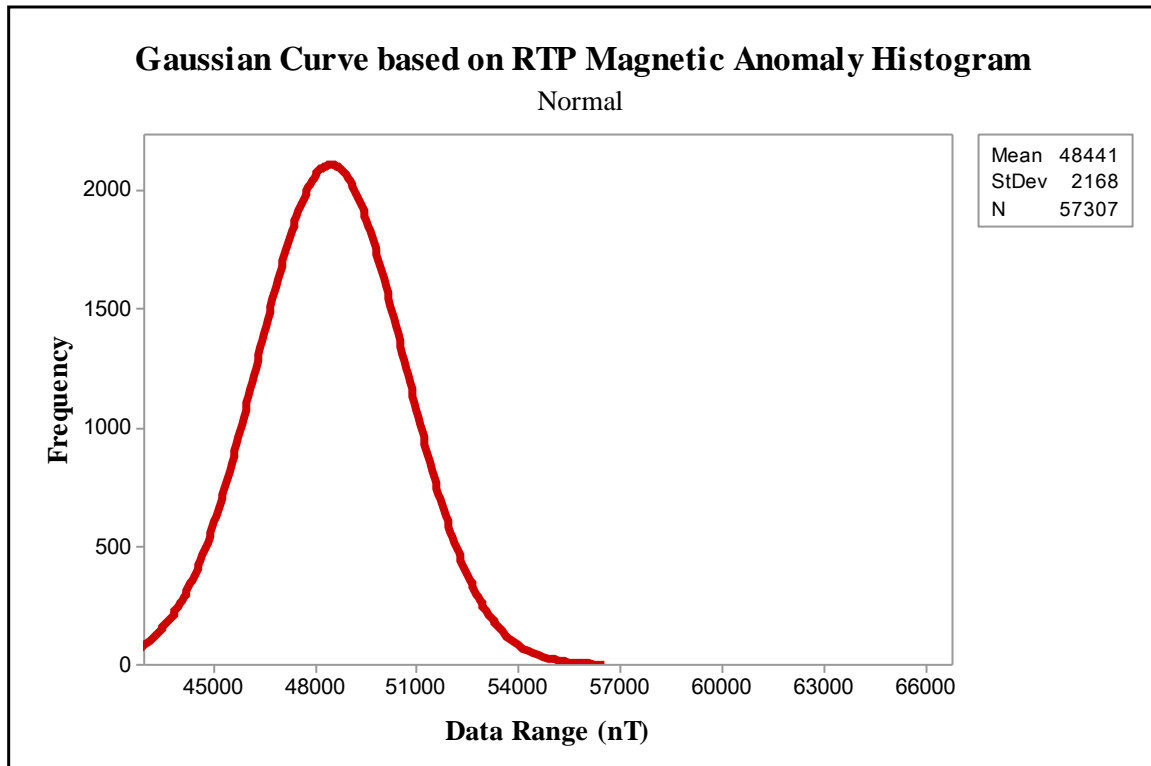
Figure 3. RTP map of Qoja-Kandi based on Reduction to the pole technique.



3 **Figure 4. Histogram of RTP-MA data in Qoja-Kandi.**

1
2
3
4
5
6
7
8
9
10
11
12
13
14
15

1



2

3

4 Figure 5. Gaussian curve based on RTP Magnetic anomaly histogram in Qoja-Kandi.

5

6

7

8

9

10

11

12

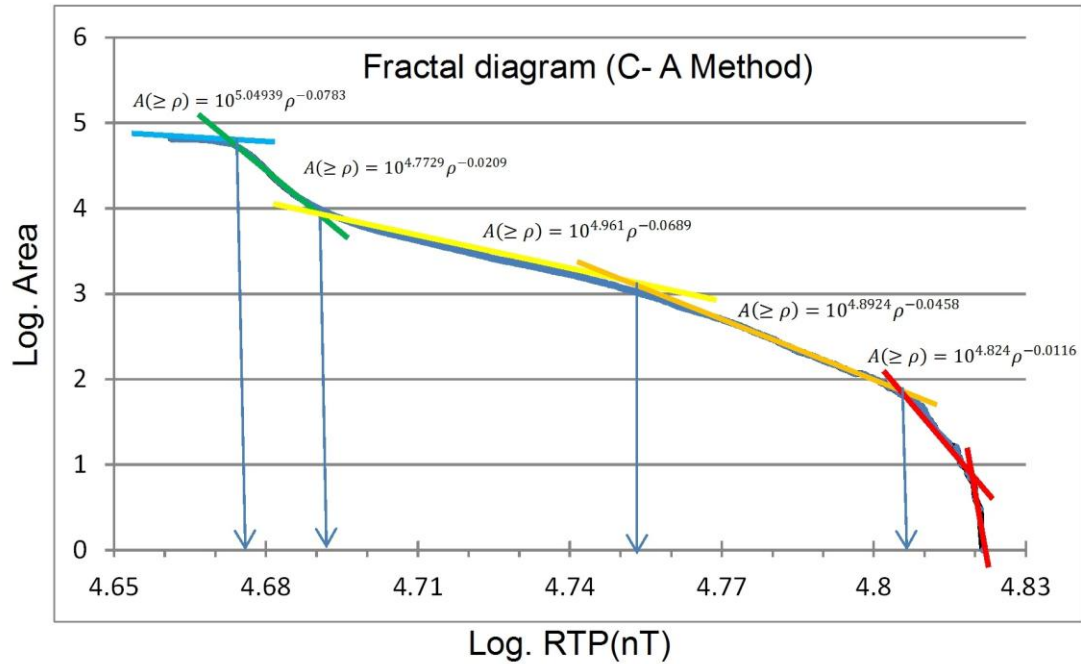
13

14

15

1

2

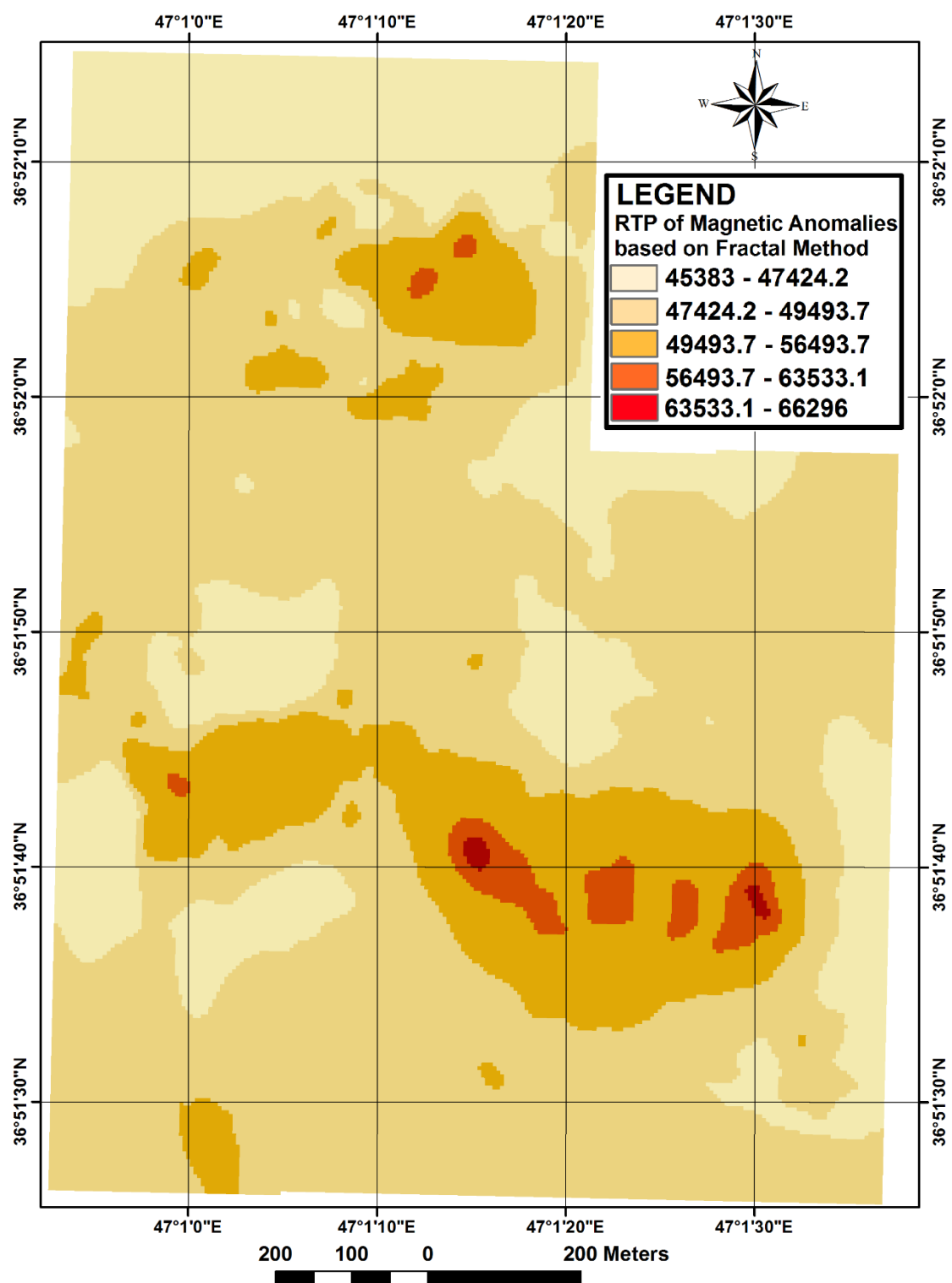


3

4

5 Figure 6. Log-log plot for RTP-MA data in Qoja-Kandi.

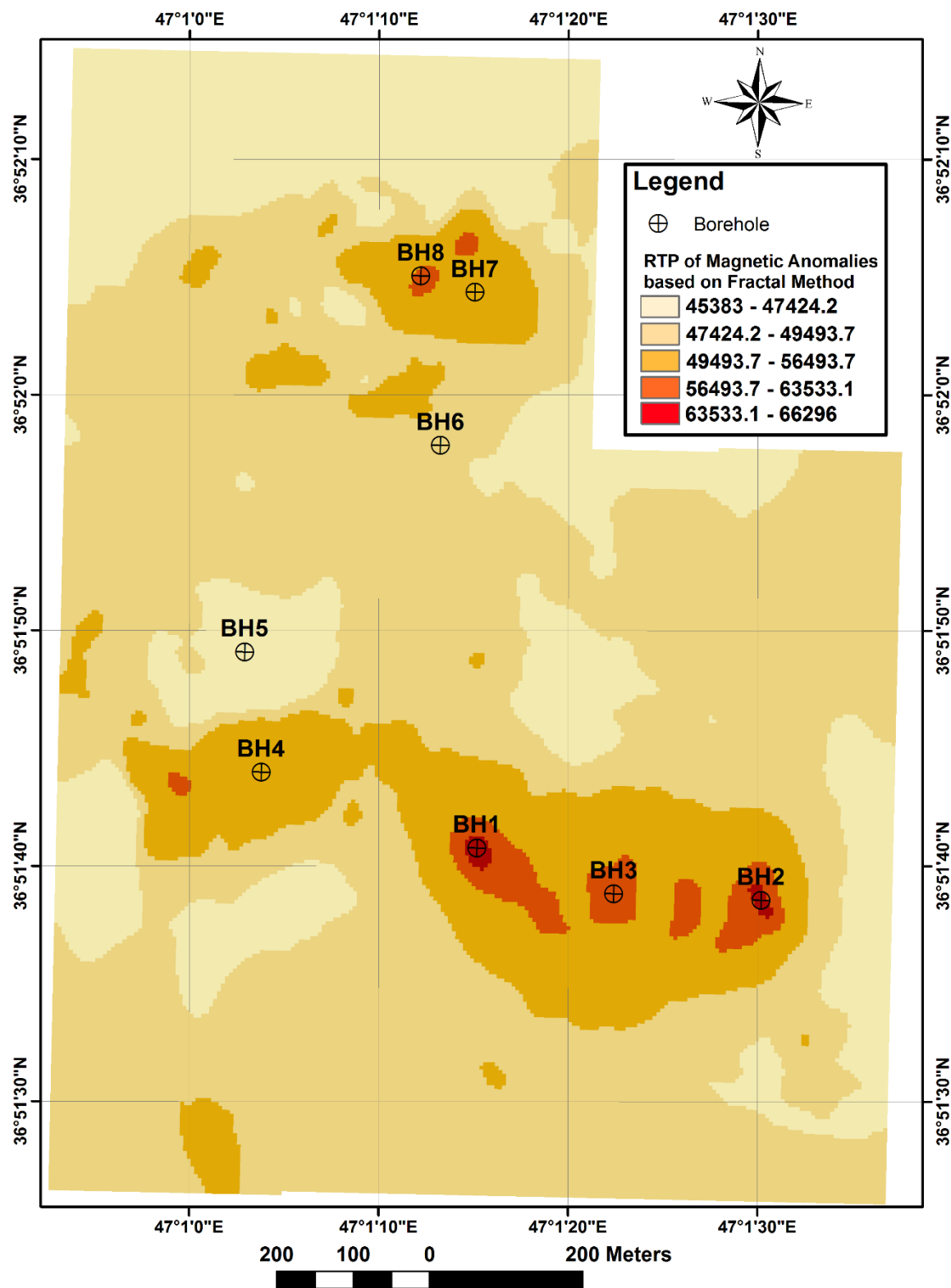
6



1

2

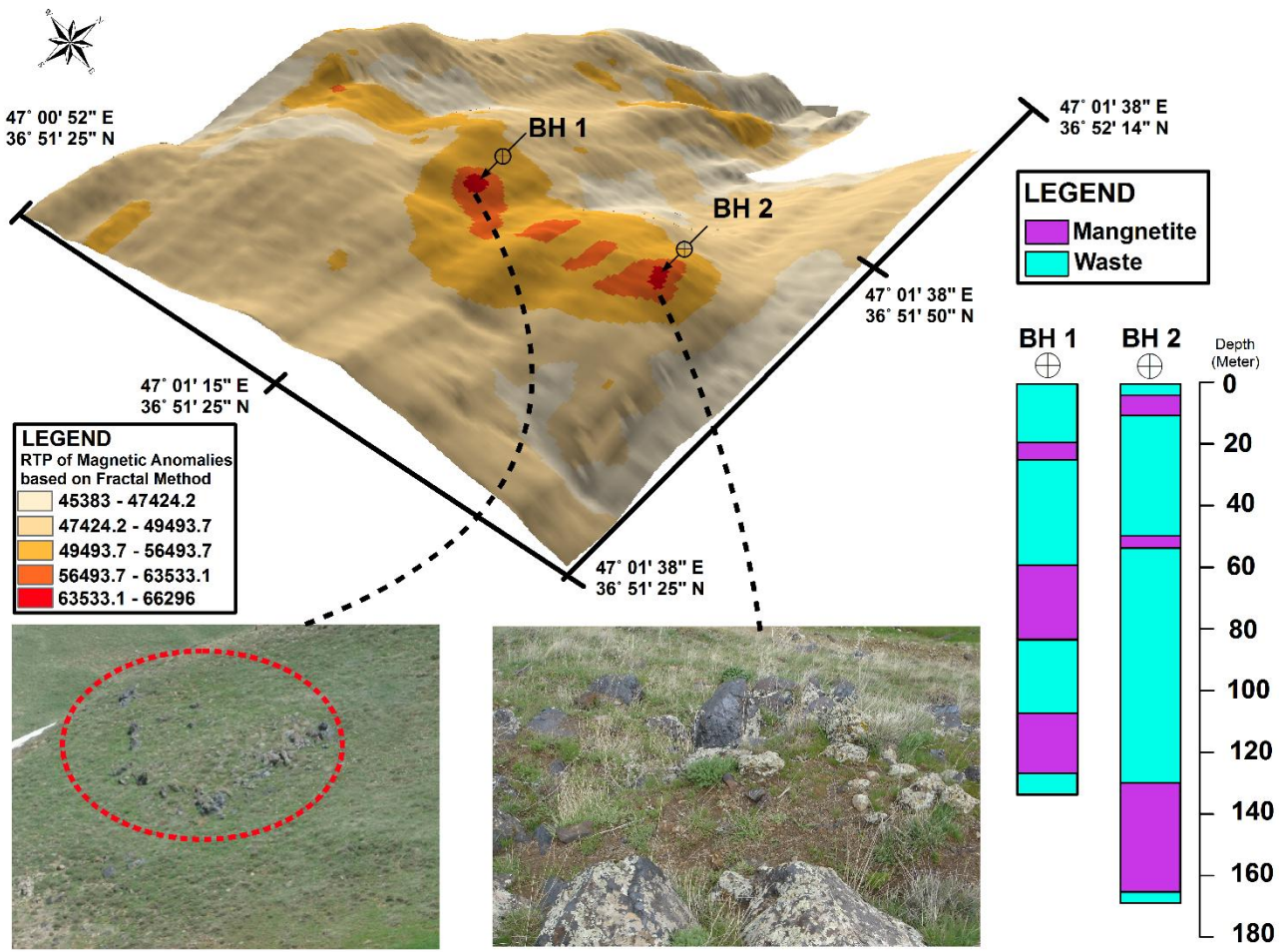
3 Figure 7. RTP map of Qoja-Kandi based on C-A method.



1

2

3 Figure 8. RTP map of Qoja-Kandi based on C-A method with drilled boreholes.



1
2

3 Figure 9. 3D RTP map of Qoja-Kandi based on C-A method with pictures from magnetite zones
4 in the surface of drilled borehole1 and 2, in addition of mentioned boreholes log plots.